DOI: 10.61782/fa.2025.0762

FORUM ACUSTICUM EURONOISE 2025

ROTOR NOISE INTERFERENCE MECHANISMS FOR SIDE-BY-SIDE CO-ROTATING CONFIGURATIONS

T. Pagliaroli[1*] **P. Candeloro**[1] **F. Del Duchetto**[1]
J. Yin[2] **K.-S. Rossignol**[2]
[1] University Niccolò Cusano, Italy
[2] DLR German Aerospace Center, Germany

ABSTRACT

This study investigates the aeroacoustic effects of phase synchronization between co-rotating propellers in side-by-side configurations. Space-time Proper Orthogonal Decomposition (POD) is applied to pressure fluctuations to separate tonal and broadband components, enabling detailed analysis of the acoustic interference phenomena. Experimental results demonstrate that synchronization significantly influences the tonal component, highlighting distinct regimes of constructive and destructive interference at different rotor phase delays. Specifically, the analysis reveals a notable reduction in noise amplitude at certain phase shifts, particularly affecting the second harmonic. An explanation of this scientific outcome is provided and illustrated schematically. Additionally, probability density functions indicate clear changes in the statistical characteristics of pressure fluctuations due to rotor synchronization, reinforcing the effectiveness of the decomposition method. These findings confirm the potential of rotor synchronization as an efficient active noise-control technique capable of achieving substantial noise reduction.

Keywords: *aeroacoustics, rotor synchronization, noise reduction, proper orthogonal decomposition, acoustic interference.*

**Corresponding author*: *tiziano.pagliaroli@unicusano.it.*

1. INTRODUCTION

U-space fosters drone integration in European airspace, yet noise pollution hinders public acceptance [1]. Studies on isolated rotor noise have intensified [2], but multirotor configurations require a broader aeroacoustic approach [1, 3, 4]. Passive noise control methods, such as serrated propeller edges, negatively affect aerodynamic performance [5], whereas active noise cancellation introduces additional weight and complexity [6]. Rotor phase synchronization emerges as a promising alternative, avoiding aerodynamic trade-offs [6]. This method manipulates rotor phase angles to induce destructive acoustic interference [7], achieving three main outcomes: noise amplitude reduction, modulation, and directivity alteration. Rotor synchronization can achieve significant noise reductions at blade passage frequency [5, 8–11], with co-rotating rotors benefiting more substantially than counter-rotating configurations [12]. Directivity modifications depend on phase differences, resulting in shifts between monopole and dipole radiation patterns [13–15]. Additionally, modulation effects introduce intermittent wave packets into pressure fluctuations [11, 14]. The present study employs space-time Proper Orthogonal Decomposition (POD) to separate the pressure fluctuation field, measured using a linear microphone array, into tonal and broadband components. This decomposition facilitates an in-depth analysis of the tonal component, typically the most annoying, offering detailed insights into the acoustic interference mechanisms between co-rotating rotors arranged in a side-by-side configuration. The paper is organized as follows. The experimental setup, instrumentation, and operating conditions are detailed in §2. Subsequently, the rotor acoustic interference phenomena are described and explained in §3. Finally, conclusions are presented in §4.

2. EXPERIMENTAL SETUP

The experiments were conducted in the Acoustic Wind Tunnel Braunschweig (AWB) optimised for noise measurements above 250 Hz. To simulate hovering conditions, the wind tunnel was deactivated during the tests. A total of 37 microphones were deployed in four non-equidistant linear arrays, with only arrays 1 and 4 used in this study. The acoustic signals were sampled at 102 kHz for 30 s per operating point. The microphone layout is illustrated in Figure 1. The setup comprised three-

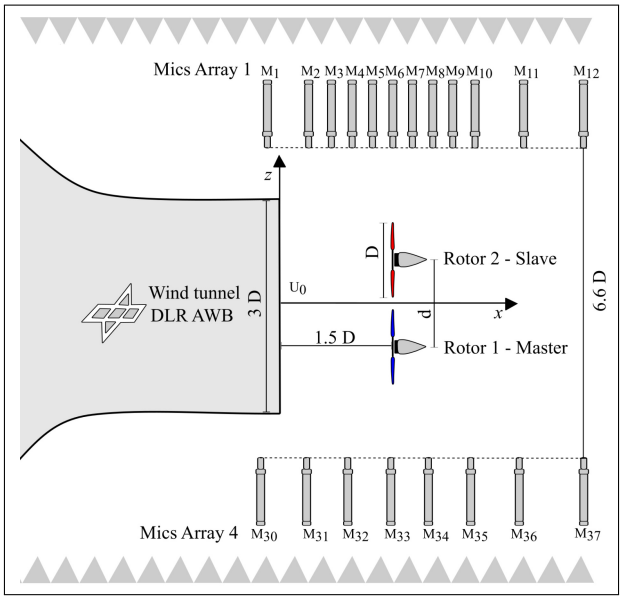

Figure 1. Microphone layout.

bladed KDE-CF155-TP propellers ($15.5'' \times 5.3$) mounted on vertical supports with adjustable spacing (d). The propellers had a diameter of 393.7 mm (D) and a mean aerodynamic chord of 28.5 mm. KDE4012XF-400 motors, controlled by KDEXF-UAS55 electronic speed controllers, powered the propellers. The two microphone arrays were positioned at $3.3D$ from the x-axis, ensuring pressure amplitudes were purely acoustic ($p' \propto 1/r$). A custom synchrophaser controlled the phase delay, $\psi(t)$, between the co-rotating rotors operating at a rotational speed $\omega(t)$. The system employed a Kübler 05.2400 incremental encoder (500 pulses per revolution) and National Instruments hardware, including an NI PXI-1031 chassis, an NI PXI-7350 motion controller, and an NI PXI-6259 multifunction DAQ. A PID controller regulated the phase shift, adjusting the slave rotor relative to the master rotor every 5 ms. The synchrophaser ensured stable rotational speeds and consistent phase differences. Experiments were conducted in hover conditions with phase differences varied in 15° increments. An inter-rotor distance was tested $d/D = 1.20$, with the rotational speed fixed at 5200 RPM. Several test cases were analysed, including an isolated rotor reference case. The blade tip Mach number was $M_{\text{tip}} = 0.31$, and the Reynolds number at 75% span was $Re_{c75} = 1.51 \times 10^5$.

3. RESULTS

The aerodynamic noise of propellers can be decomposed into two main components: tonal (narrow-band) and broadband noise. Tonal noise originates from the periodic blade motion, related directly to blade rotation speed, thickness, and aerodynamic loading. In contrast, broadband noise arises from turbulent structures and their interaction with blade edges, exhibiting random, incoherent characteristics in both space and time. The separation of these noise components is crucial for experimental analysis and validating simulations based on the Ffowcs Williams–Hawkings equation. Recent studies have introduced various separation techniques [16–19]. The space-time POD technique involves organizing collected microphone array data into limited-duration space-time fields structured into a matrix for POD analysis. The resulting modes, eigenvalues, and coefficients allow coherent and stochastic components to be separated through a truncated POD expansion. Key advantages of the space-time POD technique include ease of implementation, low sensitivity to the chosen truncation threshold and time window size, and effective performance even with relatively few microphones, aligning with common aeroacoustic experimental setups. By applying the space-time POD decomposition technique to the raw pressure data, the pressure fields were separated into tonal and broadband components. In Figure 2 the tonal component was notably smoother and perfectly in phase with the raw signal. Figure 3 illustrates the first six space-time modes, which appear pairwise. According to [20], such degeneracy, along with spatial-temporal translational symmetry, confirms the presence of travelling waves. Modes exhibit harmonic structure highlights the POD's effectiveness in isolating coherent periodic structures, aligning with harmonic orthogonal decomposition conditions discussed by [21]. Figure 4 presents the calculated Sound Pressure Spectral Level (SPSL), demonstrating that the coherent component spectrum aligns with the first three harmonics of the raw signal

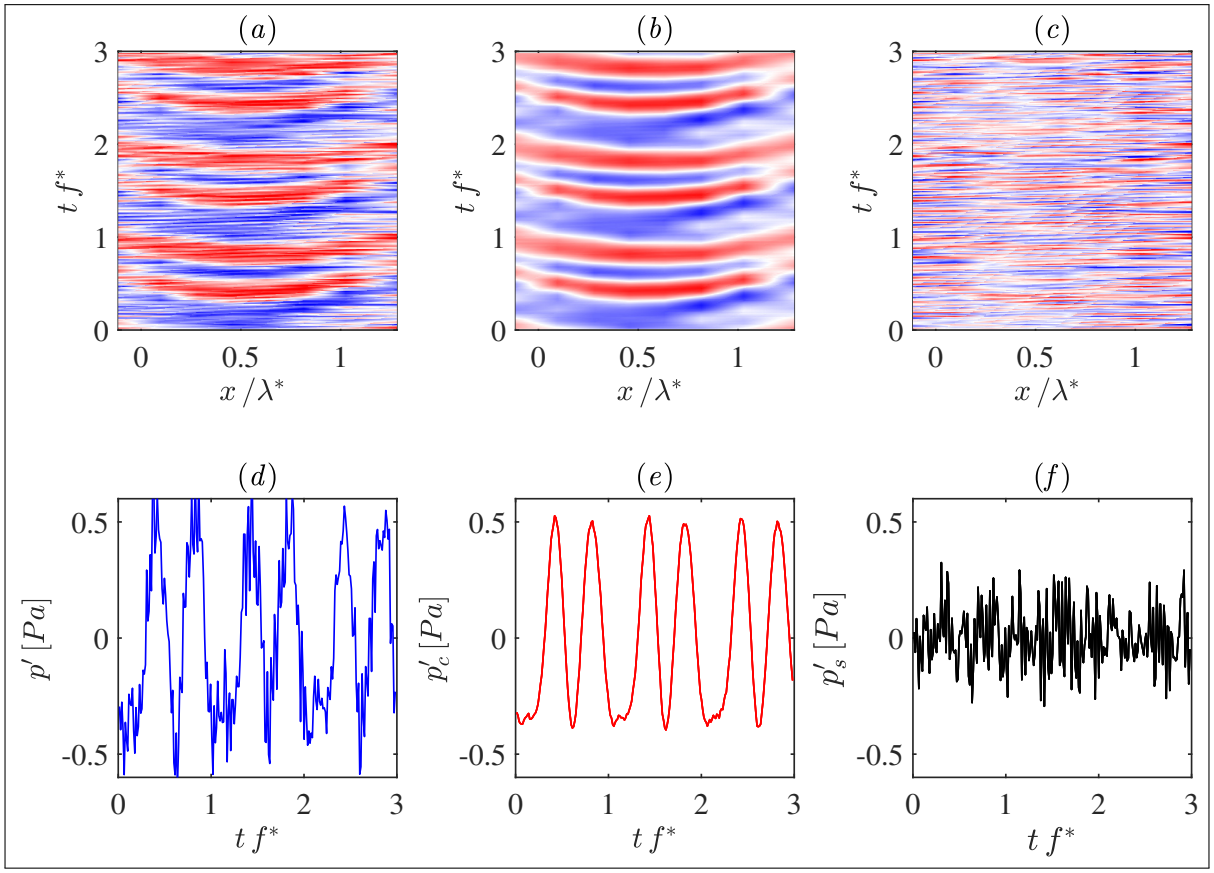

Figure 2. Input-output of the space-time POD decomposition applied to side-by-side rotor for constant phase delay $\psi = 0°$. The first column illustrates the raw data (a, d), the second column shows the tonal component (b, e), and the third column presents the broadband component (c, f). The top row represents space-time fields, while the bottom row shows a single time series at $x/\lambda^* = 0.45$, located in the rotor plane.

and remains nearly flat across the normalized frequency range $f/f^* \in [0.1, 1)$. Additionally, this decomposition technique effectively removes intermediate peaks between harmonics observed in the raw signal, distinguishing it from conventional band-pass filters. Figure 5 shows that the probability density function (PDF) of the incoherent signal closely follows a Gaussian distribution up to 3σ, confirming its stochastic nature. Conversely, the PDF of the coherent component is characterised by a bi-modal distribution, with peaks corresponding to blade passage events. These distinct PDF shapes validate the effectiveness of the decomposition technique in accurately separating tonal and broadband noise components. Figure 6 illustrates the effect of varying phase delay (ψ) between side-by-side rotors. At $\psi = 0°$ (Figure 6a), pairs of red-blue streaks appear for each blade passing period, with the delay between waves determined solely by rotor spacing. Increasing the phase delay to $\psi = 45°$ results in the alignment of compression waves from both rotors, producing constructive interference (Figure 6d). Conversely, at intermediate angles such as $\psi = 15°$ and $75°$, destructive interference occurs due to the overlap between expansion and compression waves, significantly reducing fluctuation amplitude. In Figure 7 is depicted pressure fluctuation time series showing the interference mechanism between side-by-side rotors for different phase delays (ψ). Figure 8 shows the Overall Sound Pressure Level (OASPL) for varying phase delays (ψ) between side-by-side rotors, comparing these results to the noise generated by a single rotor. This figure reveals promising findings, partic-

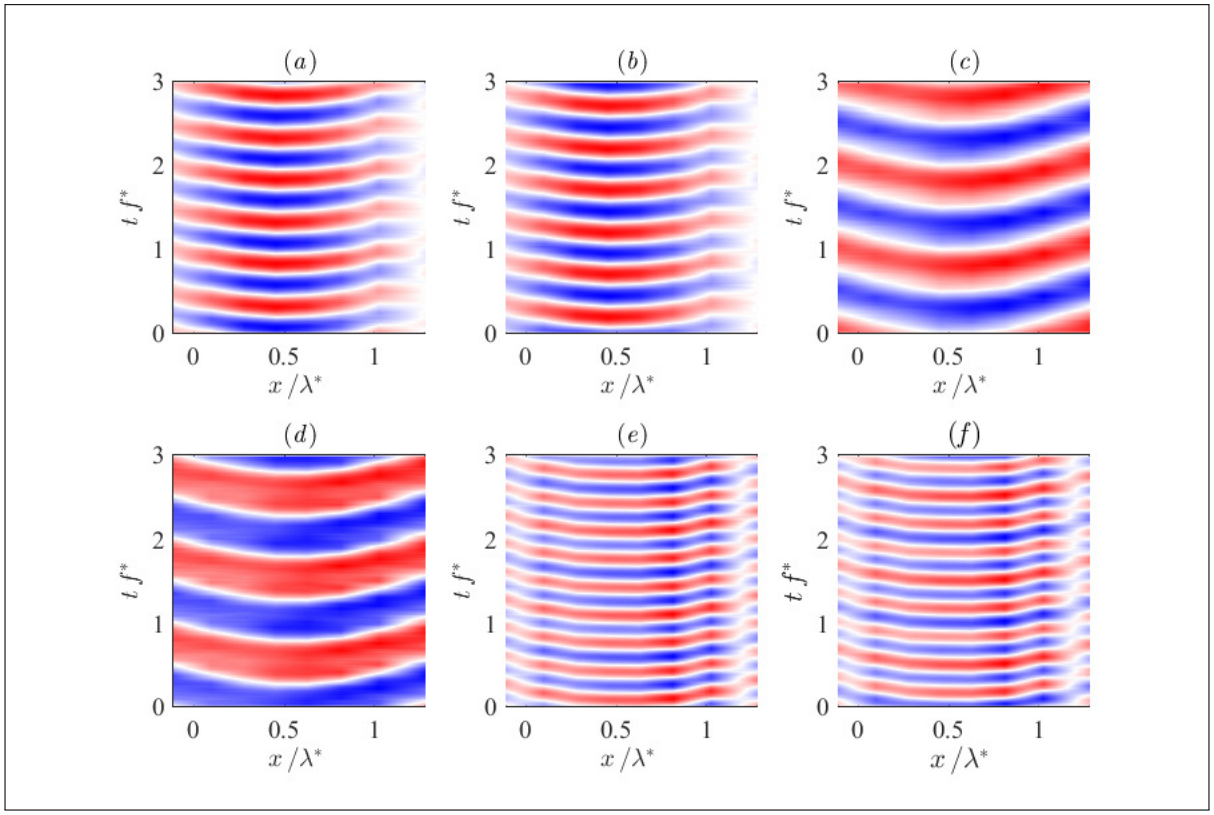

Figure 3. First six modes for side-by-side rotor for constant phase delay $\psi = 0°$ calculated using time history acquired by a linear array of microphones number 4.

ularly at angles associated with destructive interference ($\psi = 15°$ and $\psi = 75°$), where the noise produced by two synchronized rotors is notably lower than that of a single rotor. Conversely, constructive interference, observed at $\psi = 45°$, significantly increases the noise level. These findings confirm the potential of rotor synchronisation in effectively reducing aerodynamic noise through controlled interference. In Figure 9, the first harmonic is notably higher under constructive interference than in other cases. Consistent with [22], the second harmonic experiences the most significant mitigation due to destructive interference as reported in Table 1. Figure 7(f) clarifies why the second harmonic is mitigated: synchronisation of compression and expansion waves cancels fluctuations, resulting in a compression-expansion wave with reduced periodicity, as depicted by the grey-coloured fluctuation. The Probability Density Function (PDF) of pressure fluctuations provides valuable insights into how pressure signals change with varying phase delays. In Figure

Table 1. Sound Pressure spectral Level of the first and second harmonics by varying the rotor phase delay.

ψ, deg	$SPSL_1\,[dB]$	$SPSL_2\,[dB]$
0	75,3	74,4
45	82,2	82,4
75	79,6	62,4

10, at $\psi = 0°$, the PDF exhibits a distinct bi-modal distribution, clearly identifying two constant-intensity pressure fluctuations (expansion and compression). At $\psi = 45°$, these peaks shift outward, accompanied by the emergence of two lower-intensity internal peaks, ascribed to installation effects. At $\psi = 75°$, the PDF is dominated by

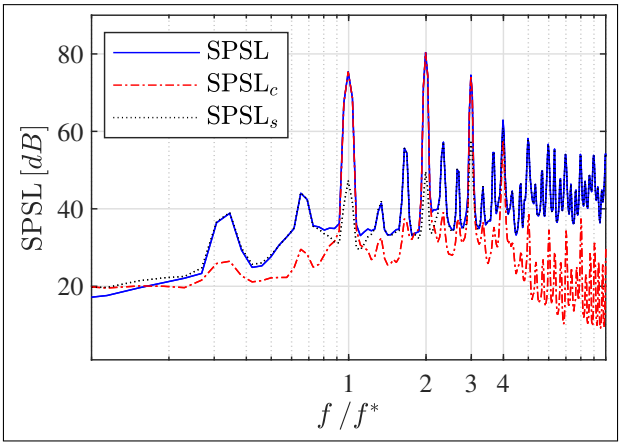

Figure 4. Sound pressure spectral levels calculated at $x/\lambda^* = 0.45$ for the raw data, tonal and broadband components.

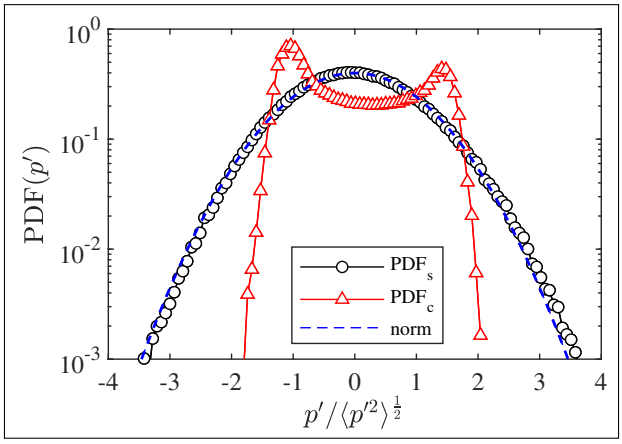

Figure 5. Probability density function of tonal and stochastic components of the pressure fluctuation.

a single expansion peak with an intensity very close to zero. This characteristic represents the acoustic footprint of noise cancellation due to destructive interference. Indeed, as illustrated in Figure 7f, the primary effect of destructive interference is the replacement of the positive-negative oscillation (see red and blue curves) with an extended sequence of values close to zero.

4. CONCLUSION

This investigation demonstrated the effectiveness of rotor phase synchronization as a passive noise reduction technique in co-rotating, side-by-side rotor configurations. Space-time Proper Orthogonal Decomposition (POD) successfully separated measured acoustic fields into tonal and broadband components, enabling precise analysis of acoustic interference mechanisms. Results revealed significant variations in noise levels due to constructive and destructive interference at specific phase angles, with notable reductions observed, particularly at second harmonic. Probability Density Function analyses confirmed clear distinctions in the statistical characteristics of pressure fluctuations, validating the decomposition technique's reliability. Overall, rotor synchronization emerged as a promising aeroacoustic control strategy, offering substantial noise mitigation potential.

5. ACKNOWLEDGMENTS

Research activities described in the manuscript are part of the work carried out by the GARTEUR AG-26 consortium, which has promoted the collaboration between DLR and Niccolò Cusano University. We sincerely thank Prof. Patanè for implementing the rotor synchronization software.

6. REFERENCES

[1] T. Dbouk and D. Drikakis, "Quadcopter drones swarm aeroacoustics," *Phys. Fluids*, vol. 33, no. 5, 2021.

[2] P. Candeloro, D. Ragni, and T. Pagliaroli, "Small-scale rotor aeroacoustics for drone propulsion: A review of noise sources and control strategies," *Fluids*, vol. 7, no. 8, p. 279, 2022.

[3] N. Intaratep, W. N. Alexander, W. J. Devenport, S. M. Grace, and A. Dropkin, "Experimental study of quadcopter acoustics and performance at static thrust conditions," in *22nd AIAA/CEAS Aeroacoustics Conference*, p. 2873, 2016.

[4] R. E. Nargi, P. Candeloro, F. De Gregorio, G. Ceglia, and T. Pagliaroli, "Fluid-dynamic and aeroacoustic characterization of side-by-side rotor interaction," *Aerospace*, vol. 10, no. 10, p. 851, 2023.

[5] B. Turhan, H. K. Jawahar, A. Gautam, S. Syed, G. Vakil, D. Rezgui, and M. Azarpeyvand, "Acoustic characteristics of phase-synchronized adjacent pro-

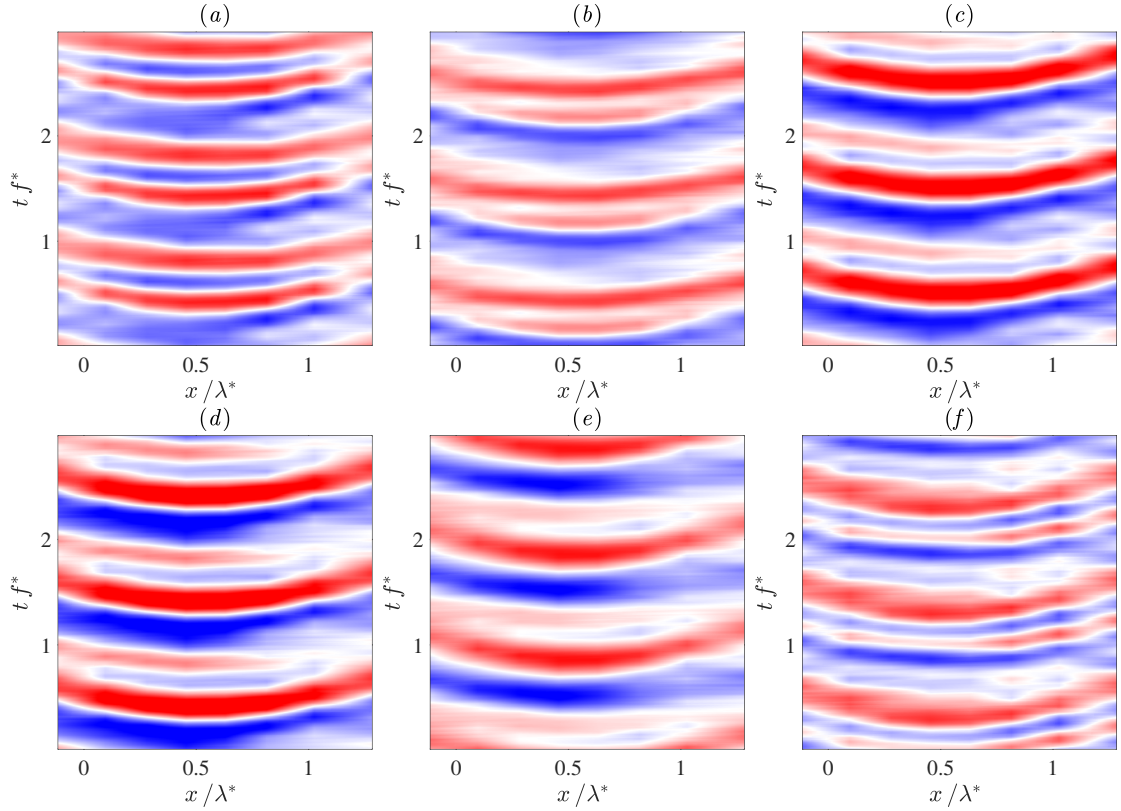

Figure 6. Pressure fluctuation space-time fields for side-by-side rotors with varying phase delays (ψ): (a) $\psi = 0°$, (b) $\psi = 15°$, (c) $\psi = 30°$, (d) $\psi = 45°$, (e) $\psi = 60°$, and (f) $\psi = 75°$.

pellers," *The Journal of the Acoustical Society of America*, vol. 155, no. 5, pp. 3242–3253, 2024.

[6] L. Chengyi, W. Yafeng, and C. Geng, "Active noise control experiment for unmanned aerial vehicle propeller," *Sci. Tech. and Eng.*, vol. 14, no. 9, pp. 1671–1815, 2014.

[7] Y. Cao, X. Huang, L. Sheng, and Z. Wang, "A flight experimental platform for synchrophasing control based on a small propeller uav," *Sci. China Technological Sciences*, vol. 61, pp. 1915–1924, 2018.

[8] A. Patterson, N. H. Schiller, K. A. Ackerman, A. Gahlawat, I. M. Gregory, and N. Hovakimyan, "Controller design for propeller phase synchronization with aeroacoustic performance metrics," in *AIAA Scitech 2020 Forum*, p. 1494, 2020.

[9] S. Guan, Y. Lu, T. Su, and X. Xu, "Noise attenuation of quadrotor using phase synchronization method," *Aerospace Sci. and Tech.*, vol. 118, p. 107018, 2021.

[10] O. Hertzman, S. Fligelman, and O. Stalnov, "Abatement of a multi-rotor tonal noise component with phase control technology," in *28th AIAA/CEAS Aeroacoustics 2022 Conference*, p. 2834, 2022.

[11] S. Zhong, P. Zhou, W. Chen, H. Jiang, H. Wu, and X. Zhang, "An investigation of rotor aeroacoustics with unsteady motions and uncertainty factors," *J. of Fluid Mech.*, vol. 956, p. A16, 2023.

[12] M. Shao, Y. Lu, X. Xu, S. Guan, and J. Lu, "Experimental study on noise reduction of multi-rotor by phase synchronization," *J. of Sound and Vib.*, vol. 539, p. 117199, 2022.

[13] K. Pascioni, S. Rizzi, and N. Schiller, "Noise reduction potential of phase control for distributed propul-

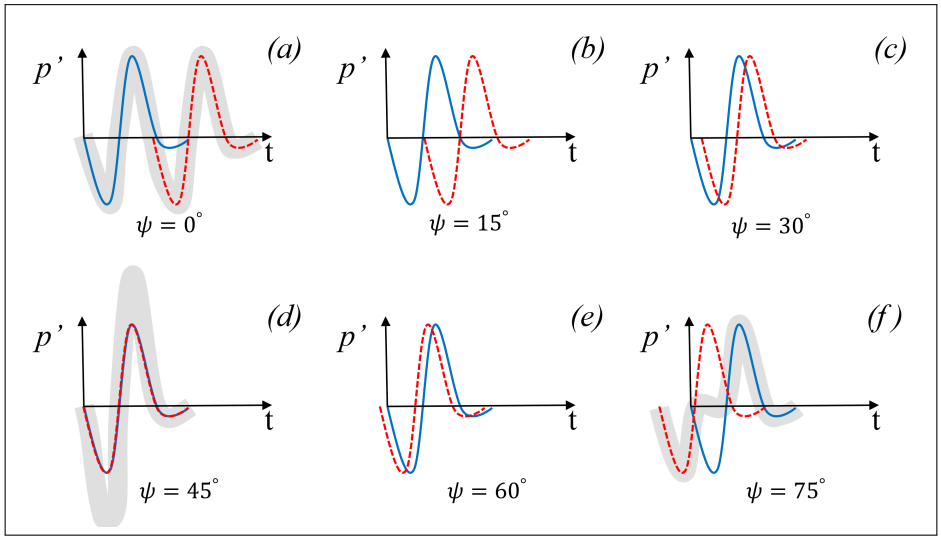

Figure 7. Schematic depiction of pressure fluctuation time series showing the interference effect between side-by-side rotors for different phase delays (ψ).

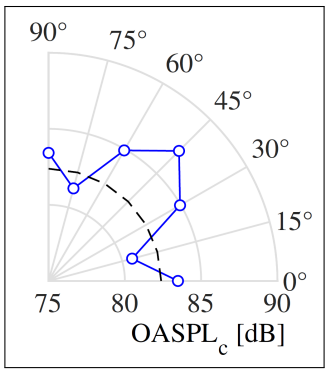

Figure 8. Overall Sound Pressure Level (OASPL) as a function of the phase delay (ψ). The dashed quarter circle represents the OASPL generated by an isolated rotor, providing a comparative reference for evaluating the effects of rotor interactions.

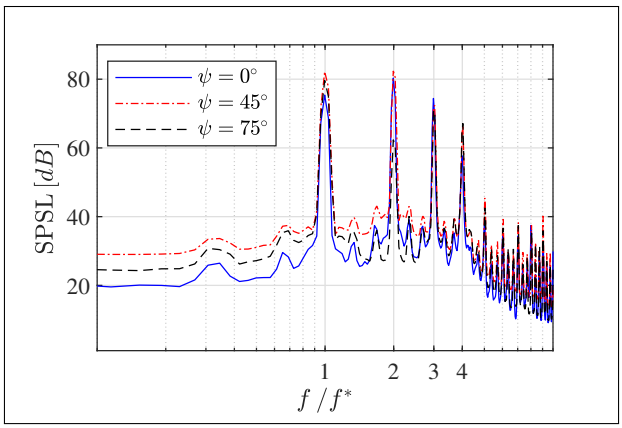

Figure 9. Sound pressure Spectra Level of the tonal component calculated for $\psi = 0°, 45°,$ and$75°$.

sion vehicles," in *AIAA Scitech 2019 Forum*, p. 1069, 2019.

[14] A. Celik, N. S. Jamaluddin, K. Baskaran, S. Meloni, D. Rezgui, and M. Azarpeyvand, "Experimental characterisation of rotor noise in tandem configuration," *Applied Acoustics*, vol. 222, p. 110053, 2024.

[15] N. Pandey, J. A. Valdez, W. Beaman, and C. E. Tinney, "Acoustics of side-by-side synchrophased rotors," in *30th AIAA/CEAS Aeroacoustics Conference (2024)*, p. 3218, 2024.

[16] L. A. Bonomo, J. A. Cordioli, A. K. Colaciti, J. V. N. Fonseca, and L. G. C. Simões, "A comparison of tonal-broadband decomposition algorithms for propeller noise," *Int. J. of Aeroacoustics*, vol. 23, no. 7-8, pp. 737–762, 2024.

[17] S. Meloni, E. de Paola, E. Grande, D. Ragni,

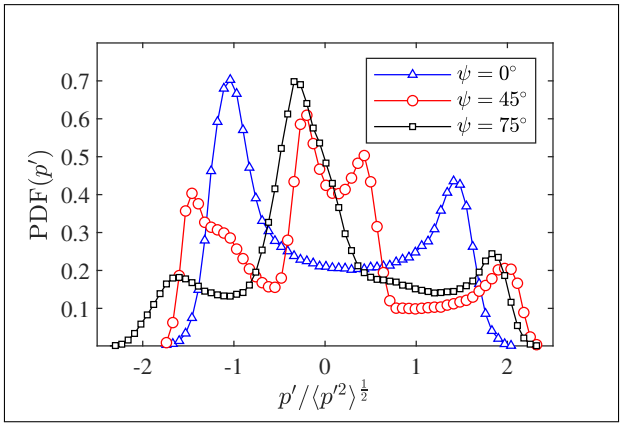

Figure 10. Probability Density Functions (PDFs) calculated ofr three condition: $\psi = 0°, 45°,$ and$75°$.

L. G. Stoica, A. Di Marco, and R. Camussi, "A wavelet-based separation method for tonal and broadband components of low reynolds-number propeller noise," *Measurement Science and Technology*, vol. 34, p. 044007, jan 2023.

[18] P. Candeloro, E. Martellini, R. Nederlof, T. Sinnige, and T. Pagliaroli, "An experimental study of the aeroacoustic properties of a propeller in energy harvesting configuration," *Fluids*, vol. 7, no. 7, p. 217, 2022.

[19] C. E. Tinney, Y. Zhao-Dubuc, and J. Valdez, "The space-time structure of sound produced by stacked rotors in hover using vold-kalman filters and proper orthogonal decomposition," *International Journal of Aeroacoustics*, vol. 22, no. 5-6, pp. 576–598, 2023.

[20] N. Hasan and S. Sanghi, "Proper orthogonal decomposition and low-dimensional modelling of thermally driven two-dimensional flow in a horizontal rotating cylinder," *J. of Fluid Mech.*, vol. 573, pp. 265–295, 2007.

[21] J. L. Lumley, "Coherent structures in turbulence," in *Transition and turbulence*, pp. 215–242, Elsevier, 1981.

[22] F. Del Duchetto, T. Pagliaroli, P. Candeloro, K.-S. Rossignol, and J. Yin, "Aeroacoustic study of synchronized rotors," *Aerospace*, vol. 12, no. 2, 2025.